The Landau–Lifshitz equation in atomistic models

M.O.A. Ellis[1], R.F.L. Evans[1], T.A. Ostler[1], J. Barker[2], U. Atxitia[3], O. Chubykalo-Fesenko[4], and R.W. Chantrell[1]

[1]*Department of Physics, University of York, York, YO10 5DD, United Kingdom*

[2]*Institute for Materials Research, Tohoku University, Sendai, Miyagi 980-8577, Japan*

[3] *Fachbereich Physik and Zukunftskolleg, Universität Konstanz, Konstanz D-78457, Germany*

[4]*Instituto de Ciencia de Materiales de Madrid, CSIC, Cantoblanco, Madrid, 28049 Spain*
E-mail: me521@york.ac.uk

The Landau–Lifshitz (LL) equation, originally proposed at the macrospin level, is increasingly used in Atomistic Spin Dynamic (ASD) models. These models are based on a spin Hamiltonian featuring atomic spins of fixed length, with the exchange introduced using the Heisenberg formalism. ASD models are proving a powerful approach to the fundamental understanding of ultrafast magnetization dynamics, including the prediction of the thermally induced magnetization switching phenomenon in which the magnetization is reversed using an ultrafast laser pulse in the absence of an externally applied field. This paper outlines the ASD model approach and considers the role and limitations of the LL equation in this context.

1. Introduction

Atomistic spin models have a long history, going back to the pioneering work of Binder [1] and co-workers in the 1970s. Typically these studies concentrated on the static properties of spin systems, particularly using Monte-Carlo methods to investigate the order/disorder phase transition and finite size effects in magnetic nanoparticles. The atomistic approach proved a powerful tool in the study of purely thermodynamic aspects of magnetic spin systems.

However, the use of atomistic models for simulating magnetization dynamics was, until recently, rather limited and generally based on Monte-Carlo simulations of escape over energy barriers. Such an approach is hampered by the fact that the timesteps are generally not quantified. Time quantification was attempted by Nowak *et al.* [2] but this is successful only in the strong damping regime where the precession can be neglected. The study of dynamic phenomena however was intrinsically limited until the development of dynamic [3,4] and stochastic atomistic spin models [5–7].

In general the model of choice for magnetization reversal studies is micromagnetics. The history of micromagnetics starts with a 1935 paper of Landau and Lifshitz on the structure of a wall between two antiparallel domains, and several papers by Brown around 1940. A detailed treatment of micromagnetism is given by Brown in his 1963 book [8]. For many years micromagnetics was limited to the use of standard energy minimization approaches to determine domain structures and classical nucleation theory to investigate magnetization reversal mechanisms in systems with ideal geometry. Arguably, the current interest in micromagnetics arises from the availability, from about the mid-1980s onward, of large-scale computing power which enabled the study of more realistic problems which were more amenable to comparison with experimental data. One important realization during this period was the fact that, although micromagnetics can predict the nucleation fields for the magnetic system, due to the coexistence of different energy minima, multiple magnetization reversal paths are possible. Thus micromagnetics does not necessarily predict the correct state of the system after magnetization reversal. Consequently, a lot of work has gone into the development of dynamic approaches which use simulations based on the Landau–Lifshitz equation of motion. This is probably the technique in most common use today.

Dynamic calculations using micromagnetics have become ubiquitous, finding applications in fundamental in-

vestigations of reversal dynamics of magnetic materials. In addition micromagnetic models are vital to many industries, including the development of new generations of magnetic recording heads and media and permanent magnets. However, limitations of the micromagnetic approach are becoming increasingly apparent. Firstly, as magnetic materials become increasingly structured at the nanoscale to investigate new physical phenomena and create new functionalities, the continuum nature of micromagnetics reaches the limits of validity. Secondly, although thermal activation can be introduced into the micromagnetic formalism, its applicability is strictly limited to low temperatures; it is known that micromagnetic models greatly overestimate the Curie temperature [9,10]. This is a serious limitation in the investigation of ultrafast magnetization dynamics, where temperatures up to and beyond T_c can be achieved on the picosecond timescale. The natural evolution is toward dynamical approaches with atomistic resolution; such models are gaining increasing traction in dealing with the physics of ultrafast magnetization processes and practical problems such as providing an understanding of heat assisted magnetic recording (HAMR) [11,12]. Remarkably, the key to atomistic spin dynamic (ASD) models is the use of the LL equation at the atomic level. Here we outline the basis of ASD models, review some recent simulations of ultrafast spin dynamics and consider the physical justification for the use of the LL equation at the atomistic level.

2. Atomistic spin dynamic models

The physical basis of the atomistic spin model is the localization of unpaired electrons to atomic sites, leading to an effective local atomistic magnetic moment, which is treated as a classical spin of fixed length. *Ab initio* calculations of the electron density [13] show that in reality, even in itinerant ferromagnets, the spin polarization is well localized to the atomic sites. Essentially this suggests that the bonding electrons are unpolarised, and after taking into account the bonding charge the remaining *d* electrons form a well-defined effective localized moment on the atomic sites. Nonetheless the assumption of classical spins leads to a fundamental discrepancy with experiments which will be discussed later.

The basis of ASD models, reviewed by Evans *et al.* [14] is a classical spin Hamilonian based on the Heisenberg exchange formalism. The spin Hamiltonian $\mathcal{H}$ typically has the form:

$$\mathcal{H} = \mathcal{H}_{\text{exc}} + \mathcal{H}_{\text{ani}} + \mathcal{H}_{\text{app}}, \tag{1}$$

with the terms on the RHS representing respectively the exchange, anisotropy and Zeeman terms. The exchange term is usually isotropic in spin space and the anisotropy term includes energies which are angular dependent. These can arise from crystalline anisotropies or magnetostriction

and strains. The exchange term can also be anisotropic in some situations as will be discussed later.

The exchange energy for a system of interacting atomic moments is given by the expression

$$\mathcal{H}_{\text{exc}} = \sum_{i \neq j} J_{ij} \mathbf{S}_i \, \mathbf{S}_j \tag{2}$$

where J_{ij} is the exchange interaction between atomic sites i and j, $\mathbf{S}_i$ is a unit vector denoting the local spin moment direction and $\mathbf{S}_j$ is the spin moment direction of neighboring atoms. The unit vectors are taken from the actual atomic moment $\boldsymbol{\mu}_i$ and given by $\mathbf{S}_i = \boldsymbol{\mu}_i / \mu_s$ where μ_s is the saturation magnitude of the atomic moment. Due to the strong distance dependence of the exchange interaction the sum in Eq. (2) is often truncated to include nearest neighbors only. This significantly reduces the computational effort while being a good approximation for many materials of interest. In reality the exchange interaction can extend to several atomic spacings [15,16], representing hundreds of pairwise interactions.

In the simplest case the exchange interaction J_{ij} is isotropic, meaning that the exchange energy of two spins depends only on their relative orientation. In more complex materials, the exchange interaction forms a tensor with components:

$$\mathbb{J}_{ij} = \begin{bmatrix} J_{xx} & J_{xy} & J_{xz} \\ J_{yx} & J_{yy} & J_{yz} \\ J_{zx} & J_{zy} & J_{zz} \end{bmatrix}, \tag{3}$$

which is capable of describing *anisotropic* exchange interactions, such as two-ion anisotropy [15] and the Dzyaloshinskii–Moriya interaction (off-diagonal components of the exchange tensor). In the case of tensorial exchange, the exchange energy is given by the product:

$$\mathcal{H}_{\text{exc}} = -\sum_{i \neq j} \mathbf{S}_i^T \mathbb{J}_{ij} \mathbf{S}_j. \tag{4}$$

We now proceed to consider two important factors in the use of ASD, firstly the process of determining, from first principles, the parameters of the spin Hamiltonian and secondly the introduction of spin dynamics, and the implications of the use of the LL equation at the atomistic level.

2.1. Ab-initio calculation of spin Hamiltonian parameters: Multiscale approaches

The material parameters central to the spin Hamiltonian are the exchange interactions, anisotropy energies, and the magnitude of the spin moment. These can generally be found using two routes: (i) experimental measurements, either in a mean-field sense from macroscopic quantities such as the Curie point, or microscopically using neutron scattering, (ii) with a multiscale approach using *ab initio* density functional theory (DFT) calculations to parameterise

the spin model. The *ab initio* approach is often preferable as it removes extrinsic factors from the parameters such as nonuniformity of an experimental sample and also provides a resolution (for example many exchange neighbours) which is hard to obtain experimentally even with neutron scattering. Difficulties can arises such as in magnetic materials involving rare-earths, where the treatment of the 4*f* electrons is problematic in DFT. In this case an experimental parameterization becomes the most practical route, as was done by Ostler *et al*. [17] for amorphous GdFeCo alloys and Evans *et al*. [18] for $Nd_2Fe_{14}B$ alloys.

Contemporary *ab initio* methods enable the calculation of a wide range of material properties including ground state magnetic properties. So-called "beyond DFT" methods allow the calculation of even small energy differences, providing access to the magnetic crystalline anisotropy constants. Standard software packages such as VASP [19] and SIESTA [20] make such calculations accessible to interested researchers. The calculation of pair wise exchange interactions in DFT is somewhat complicated by the delocalised nature of the basis sets employed. Parameterizing a spin Hamiltonian therefore requires mapping many different spin configurations onto the atomic Hamiltonian. An alternative is to use scattering methods such as Korringa–Kohn–Rostoker [21,22] or linear muffin tin orbitals [23,24]. These methods are built around the atomic sphere approximation which gives a natural mapping onto the localised Heisenberg formalism in conjunction with the magnetic force theorem [25].

Connecting the *ab-initio* and atomistic length scale is an important link in the mulultiscale modelling chain allowing one to include both dynamics and temperature, which has been demonstrated for FePt by Kazantseva *et al*. [26]. In this section we consider the calculation of the temperature dependence of static materials properties. Mryasov *et al*. [27] carried out *ab-initio* calculations of exchange and anisotropy of the L_1O phase of FePt; an important candidate for HAMR media. The aim was to investigate the exchange and anisotropy values of bulk FePt and to map them onto a classical spin model in order to investigate static and dynamic properties. This process was complicated by the induced Pt moments arising from the Fe exchange field. Such an effect is beyond the Heisenberg model of fixed moments, but based on *ab-initio* calculations an effective spin Hamiltonian was developed which is dependent only on the Fe degrees of freedom.

$$\mathcal{H}^{FePt} = -\sum_{i \neq j} (\tilde{J}_{ij}\mathbf{S}_i \cdot \mathbf{S}_j + \tilde{D}_{ij}^{(2)} S_i^z S_j^z) - \sum_i \tilde{D}_i^{(0)} (S_i^z)^2. \quad (5)$$

The exchange parameters include the effect of Fe–Pt–Fe interactions which contributes to both the isotropic exchange $\tilde{J}_{ij}$ as well as introducing a two-ion anisotropy, $\tilde{D}_{ij}^{(2)}$, because of the layered ordering of this intermetallic compound. This two-ion term is considerably larger than

the single ion anisotropy $\tilde{D}_i^{(0)}$. The exchange interactions are significant over large distances, making numerical calculations rather time consuming. Physically it leads to strong finite size effects [28] and in particular leads to deviations of the finite size scaling exponents from the expectations of the nearest neighbour Heisenberg form [29–31].

In Ref. 27, the thermodynamic properties of FePt were investigated using an atomistic model based on the spin Hamiltonian given in Eq. (5). It was shown that the two-ion term gives rise to a thermal anisotropy scaling exponent $n = 2$ (with $K(T) \propto M^n(T)$) consistent with the theory of Callen and Callen [32] and in contrast to the single ion anisotropy for which the exponent is $n = 3$. The importance of the atomistic approach is that it is able to calculate the exact exponent arising from the specific material parameters of FePt. This resulted in $n = 2.1$, the non-integer value reflecting the relative importance of the single- and two-site anisotropy terms; a value in good agreement with experiments on FePt nanoparticles [33,34].

2.2. Langevin dynamics and the LL equation at the atomic level

The important step forward in the use of atomistic models is the introduction of Langevin dynamics, allowing modelling of the dynamical response of the magnetization to temperature changes [35]. The approach is based on the introduction of thermal fluctuations for a single particle developed by Brown [36]. The theoretical basis is the classical theory of Brownian motion which accounts for the departure from thermal equilibrium due to the energy interchange between a particle and its heat bath, with the Landau–Lifshitz equation augmented by white-noise fields, effectively producing the stochastic (Langevin) equation of the problem. The approach is to determine local fluctuating fields using the fluctuation dissipation theorem and to require the equilibrium distribution function of the orientations of the magnetization to coincide with the Boltzmann distribution.

In order to yield the Boltzmann equilibrium distribution, the stochastic LL equation should be interpreted as a Stratonovich vector stochastic differential equation [37]. This is integrated by a suitable choice of the numerical integration scheme, most usually that of Heun. Care must be taken that the spin moments remain of unit length and for a nonconservative scheme such as Heun, an explicit renormalization of the length at each timestep is required for the Stratonovich solution [38]. The integration of the stochastic LL equation is discussed in detail in Ref. 14.

Consequently, the basis of ASD for a set of coupled spins is the integration of the stochastic Landau–Lifshitz equation for each localized magnetic moment $\mathbf{S}_i$:

$$\dot{\mathbf{S}}_i = -\gamma[\mathbf{S}_i \times \mathbf{H}_i] - \gamma\alpha[\mathbf{S}_i \times [\mathbf{S}_i \times \mathbf{H}_i]]. \quad (6)$$

Here $\mathbf{H}_i = \boldsymbol{\xi}_i(t) - d\mathcal{H}/d\mathbf{S}_i$ is the local effective field which includes Zeeman, exchange, anisotropy and magnetostatic contribution, augmented with a stochastic term $\boldsymbol{\xi}_i(t)$ (which appears like a field). It is defined through the correlators:

$$\langle \xi_i(t) \rangle = 0, \quad \langle \xi_{i\eta}(t)\xi_{j\nu}(t') \rangle = \frac{2\alpha k_B T}{\gamma\mu_s}\delta(t-t')\delta_{ij}\delta_{\eta\nu}. \quad (7)$$

Here T is the temperature of the heat bath, γ is the gyromagnetic ratio, μ_s is the magnetic moment, α is the parameter describing the coupling strength to the heat bath, η and ν are Cartesian components. The basis of this equation is the separation of timescales, assuming that the bath (phonon or electron system) is much faster than the spin system. Consequently, the fluctuation-dissipation theorem can be applied to derive the equilibrium white noise properties of Eq. (7). In Section 4 we consider the applicability of the Langevin dynamic approach using the LL equation. However, prior to this we give some examples of the success of ASD models in developing an understanding of the thermodynamic aspects of ultrafast magnetization processes, including the prediction of a novel "linear" reversal mechanism.

3. Atomistic models of ultrafast spin dynamics

Advanced models are required in order to understand ultrafast magnetization processes. Interest in this area has developed rapidly since the experimental demonstration [39] that the magnetization of Ni can be reduced by laser heating on a timescale of l ps. Experimentally the measurements are made using a pump-probe process. A high energy femtosecond laser is used to heat the material (pump), and the magnetic response is measured using magneto-optical Kerr effect (MOKE) with a low energy probe beam split off from the pump. This experiment gives time resolved measurements of the magnetic response following pulsed laser heating. Such experiments are extremely challenging in terms of understanding the physics of ultrafast magnetization processes and damping mechanisms.

A more recent development was the experimental demonstration by Stanciu *et al*. [40], of optically induced magnetization reversal in the amorphous ferrimagnet GdFeCo. Using circularly polarised ultrafast laser pulses, Stanciu *et al*. showed magnetization reversal to be dependent on the chirality of the laser pulse. This was interpreted as arising from a large, laser-generated, opto-magnetic field (estimated as large as 20 T) possibly originating from the inverse Faraday effect, the reversal was explained [41] using atomistic and Landau–Lifshitz–Bloch (LLB) macrospin simulations (for a review of the LLB equation see [42]) as arising from this large optomagnetic field together with a purely thermodynamic contribution which initiates switching via the so-called linear reversal mechanism [43]. Linear reversal is an important prediction of the

atomistic model and property of the LLB equation. Essentially it involves a collapse of the magnetization to zero and subsequently a switched polarisation in a reversing field. Linear reversal sets in at a critical temperature T^* related to the ratio of the longitudinal and transverse susceptibilities [43]. Importantly, this leads to ultrafast magnetization reversal since the timescale is governed by the longitudinal relaxation time which is of the order of hundreds of femtoseconds.

Originally optomagnetic switching was only observed in various ferrimagnetic structures but it can, in principle, occur in ferromagnets as well. The experimental work by Lambert *et al*. [44] found that thin films of ferromagnetic Co/Pt layers and granular FePt showed magnetization switching after repeated excitation by a circularly polarised femtosecond laser. Figure 1 shows an atomistic model simulation of the response of the magnetization of FePt to the field and temperature pulses associated with a femtosecond laser pulse. The calculations used the spin Hamiltonian of Mryasov *et al*. [27] given in Eq. (5) with a optomagnetic
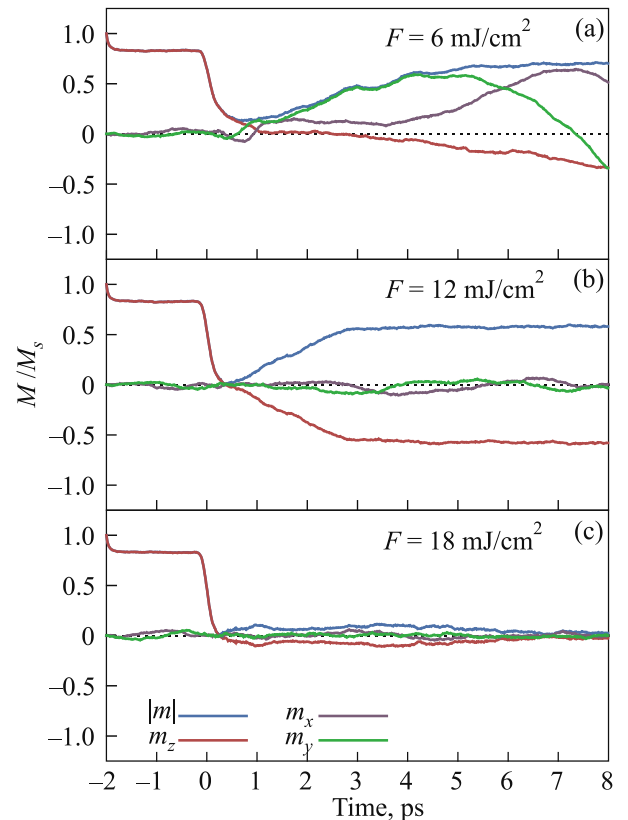

Fig. 1. (Color online) The temporal evolution of the magnetization in FePt after a femtosecond laser pulse simulated using the atomistic model described in Sec. 2. The model uses the Hamiltonian expressed in Eq. 5 with a damping, $\alpha = 0.1$, and $\mu_s = 3.23\ \mu_B$ The system starts at room temperature before excitation by a 100 fs laser pulse incident at t = 0 ps with fluences of (a) 6 mJ/cm^2 (b) 12 mJ/cm^2 and (c) 18 mJ/cm^2. A reversing optomagnetic field also occurs with the laser pulse; it has a square pulse shape from t = 0 ps to t = 1 ps with a magnitude of 30 T.

field of 30 T that lasts for 1 ps after laser excitation. The dynamic response is calculated using Langevin dynamics driven by the electron temperature evolved using a 2-temperature model [45]. The reversal depends critically on the laser power, as shown in Fig. 1. At low laser power, Fig. 1(a), demagnetization is not complete and the reversal proceeds via the usual precessional route, albeit over an energy barrier reduced due to the quenching of the anisotropy. Complete reversal proceeds over many picoseconds. At elevated temperatures, Fig. 1(b), switching of the total magnetization proceeds by a process involving no macroscopic precession; the linear reversal mode. Importantly, switching via the linear reversal mode occurs on a timescale of the longitudinal relaxation time of the magnetization (~hundreds of fs). At higher laser power, Fig. 1(c), reversal occurs but the magnetization is destroyed by the elevated temperature. Vahaplar *et al.* [41] show that optically induced switching proceeds above a critical temperature which is sufficient to excite linear reversal but not so large as to demagnetize the system.

It was shown by Vahaplar *et al.* [41] that extremely high optically-induced fields (tens of Tesla) needed to be invoked to trigger the all-optical reversal. The possible origin of such fields remains a matter of debate. However, it can be shown that the fields may arise from interatomic exchange forces. This interpretation begins with the observation by Radu *et al.* [46] that the RE and TM sublattices demagnetize at different rates, even though strongly coupled through intersublattice exchange forces. The measurements were made using XMCD (x-ray magnetic circular dichroism) to provide the element specific magnetization dynamics. The experimental observations were supported by atomistic model calculations, which verified both the differential sublattice dynamics and the existence of an intriguing transient ferromagnetic-like state (TFMLS) which is created by the reversal of the TM spins into the RE spin direction. The TFMLS exists for around 500 fs and is associated with the magnetization reversal process. Further investigation led to the astonishing prediction by Ostler *et al.* [47], using atomistic model calculations that switching occurred *in the absence of any external symmetry breaking field*. In Ref. 47 this remarkable prediction was verified experimentally. Interestingly, thermally induced magnetization switching (TIMS) allows a reinterpretation of optically-induced magnetization reversal. Rather than invoking large fields of opto-magnetic origin, Khorsand *et al.* [48] gave experimental evidence in favour of TIMS as the main switching mechanism in GdFeCo and attribute the helicity dependence of the laser excitation on the dichroic effect, i.e. the dependence of the absorption of energy from the laser pulse on the chirality of the laser light.

The phenomenon of TIMS has been further investigated theoretically using macrospin models [49,50] and atomistic approaches [51]. Importantly, Refs. 50 and 51 show that TIMS arises from angular momentum transfer between the RE and TM sublattices mediated by the establishment of a two-magnon bound state. The study in Ref. 51 involved detailed calculations of the magnon band structure, which has two branches with properties which strongly depend on the material composition. Calculations showed that transfer of energy between the modes, resulting from laser excitation, was the physical origin of the TIMS phenomenon. Further, the calculations demonstrated a window for TIMS within a certain range of alloy concentrations. Specifically, for low RE concentration essentially a uniform FM mode is excited. With increasing RE concentration, the optical mode becomes accessible, leading to TIMS. At higher RE concentrations there develops a large band gap which precludes the angular momentum transfer between sublattices, at which point TIMS cannot be excited. This prediction is in good agreement with experiment.

The results of Ref. 51 allow the definition of design rules for TIMS. Specifically,

1. The existence of two sublattices with differential demagnetization dynamics.

2. Antiferromagnetic coupling between the sublattices.

3. Reversal of the dominant magnetic sublattice which stabilises the switched magnetization direction during the cooling phase following the laser pulse.

This gives rise to the expectation that synthetic ferrimagnetic (SFIM) structures consisting of two ferromagnetic layers separated by an element such as Ru or Ir, to establish AF coupling between the layers, would exhibit TIMS. This has been demonstrated numerically by Evans *et al.* [52] in bilayers of Fe and FePt coupled by an exchange separation layer assumed to promote AF coupling between the FM layers. Importantly, this extends the TIMS phenomenon beyond its initial prediction and discovery in amorphous ferrimagnets [47] to designed materials with high anisotropy and the avoidance of RE components. This is of importance both in terms of fundamental understanding of ultrafast magnetization processes and of applications in information storage. In the latter context we note that Evans *et al.* [53] demonstrated the requirement for large write fields in the magnetic recording process; not simply to ensure magnetization reversal, but also that there is no back-switching of the magnetization, which would lead to a limiting source of noise. Ostler *et al.* [47] show that extremely large fields ~ tens of Tesla are necessary to oppose the formation of the TFMLS. This is consistent with the physical origin of TIMS in the excitation of the two-magnon bound state, which naturally introduces fields arising from the exchange interaction.

Clearly, TIMS is an important prediction using a model based on LL dynamics at the atomistic level and shows the LL equation to be a remarkable piece of insight which finds application at time- and length-scales significantly beyond its original conception. In the following we consider the underlying physics of the LL equation at the atomistic level, distinguishing between the origin of the precession and damping terms.

4. Analysis of the atomistic Langevin dynamic approach using the LL equation

The precession term in the LL equation derives directly from the equation of motion

$$i\hbar \frac{d}{dt}\langle M \rangle = \langle [M, \hat{H}] \rangle, \qquad (8)$$

with $\hat{H} = -M \cdot B(t)$, which leads directly to the Larmor precession term. The damping term is more difficult to justify at the atomistic level. Pragmatically one can make the case that some term coupling the spin to the heat bath is necessary to ensure eventual thermal equilibrium with the heat bath. In this spirit, the LL damping term is the simplest form capable of including this key physical requirement. Some work has been carried out to investigate spin dynamics at the quantum level. In particular, Cappelle and Gyorffy [54] have investigated magnetization dynamics using time dependent density functional theory. They construct a gradient-dependent density functional which is then used to derive the phenomenological LL form of damping directly from first principles. The LL equation and its damping term can also be derived from the quantum mechanics using the density matrix formalism [55], an approach recently revisited by Weiser [56]. The coupling of the spin to the heat bath is expected to be material dependent; essentially it represents the relevant energy transfer channel which might arise from interaction between the spin and conduction electron or spin/lattice interactions and should be studied at the quantum level.

The introduction of thermal fluctuations into the atomistic model formalism is achieved via the Langevin dynamic approach. As mentioned previously, the assumption is made that the instantaneous random fields, by which the thermal fluctuations are introduced, are uncorrelated in time and space, giving rise to white noise. The basis of this formalism is the separation of timescales, assuming that the bath (phonon or electron system) is much faster than the spin system. In this case, the bath degrees of freedom can be averaged out and replaced by a stochastic field with white noise correlation functions. In a sense this is perhaps the most questionable part of the application of the atomistic model in ultrafast magnetism, which involves phenomena on the timescale of tens of femtoseconds, where spatial and temporal noise correlations might be expected.

Investigation of this phenomenon is the province of models simulating the thermal behavior of the heat bath and coupling this to the spin system. In this case only the precession term of the LL equation is retained, with the damping included via a term based on the underlying mechanism coupling the spin to the heat bath. This was treated in a generic way by Atxitia *et al*. [57] using an approach developed by Miyazaki and Seki [58] and generalising this to multi-spin systems. The noise takes the form of an Ornstein–Uhlenbeck process [59] introducing a char-

acteristic correlation time τ_c. The spin is coupled locally to the bath which is connected to a thermostat as follows

$$\dot{\mathbf{S}}_i = \gamma \left[\mathbf{S}_i \times \left(\mathbf{H}_i + \boldsymbol{\eta}_i \right) \right], \qquad \dot{\boldsymbol{\eta}}_i = -\frac{1}{\tau_c}(\tau_i - \chi \mathbf{S}_i) + \mathbf{R}_i, \qquad (9)$$

with the fluctuation–dissipation theorem for the bath variable: $\langle \mathbf{R}_i(t) \rangle = 0$; $\langle \mathbf{R}_i(t) \mathbf{R}_j(t') \rangle = (2\chi k_B T / \tau_c) \delta_{ij} \delta(t - t')$. The parameter χ describes the coupling of the bath variable to the spin. The precession term in the first equation of the set (9) has the same form as in the Eq. (6). However, the damping is now described by the second equation in this set. In the second equation in Eqs. (9) the bath variable adjusts to the direction of the spin due to the interaction with it. In the limit $\tau_c \to 0$ the stochastic LL equation (6) is recovered. This also provides a relation between the damping and the coupling constants as $\alpha = \gamma \chi \tau_c$, giving a more precise physical sense to the LL damping constant at the atomistic level.

In this approach, the phenomenological LL damping parameter is substituted by two unknown parameters: the correlation time τ_c and the coupling constant χ. Several processes may be important in determining these constants, for example, the spin-orbit coupling, momentum relaxation, scattering rate and dephasing time of conduction electrons. As in the LL approach, these parameters will be material specific and their physical origins should be clarified on the basis of first-principles approaches. The effect of the correlation time on the ultrafast demagnetization process was investigated in Ref. 57. For a correlation time $\tau_c < 1$ fs the correlated approach gives the same results as the standard Langevin dynamics with white noise. However, in the range $\tau_c \simeq 10$–100 fs the correlations were found to give a dramatic increase of the longitudinal relaxation time. The effect is less pronounced at higher temperature since in this case the temperature contributes to the loss of correlations. Calculations based on the Langevin dynamics approach generally give reasonable values for the longitudinal relaxation time in comparison with experiment, which suggests that experimental correlation times are on the order of 10 fs or less; greater values would have an appreciable effect on the observed rates of demagnetization.

The interactions of the spins with the lattice system also provides an energy channel for the fluctuation and dissipation. In conventional atomistic models the lattice is fixed and so transfer to and from the lattice is handled phenomenologically by the fluctuation and damping terms in the stochastic LL equation. By introducing the motion of the atoms to the model the energy transfer can be modelled directly without the need for the phenomenological terms. Recently models such as this have been developed to investigate a variety of systems where the spin-lattice effects are important. Ma *et al*. [60] have extensively developed a spin-lattice model of Fe that utilises the dependence of the exchange on the atomic separation as the coupling between the spins and lattice. However in this case both the spins

and lattice use a Langevin thermostat to maintain a constant temperature. Through this model both systems act as a thermal reservoir from which instantaneous spin and lattice temperatures can be extracted which can then be dynamically linked to the electron temperature thus representing a dynamic three temperature model [61]. Using this model, termed spin-lattice-electron dynamics (SLED) by Ma *et al.*, experimental ultrafast laser induced magnetization dynamics can be reproduced.

Whilst the exchange interaction can couple the spins and lattice further coupling terms have also been investigated. Karakurt *et al.* [62] implemented a spin-lattice model where the exchange is constant but introduce a specific coupling term of the form:

$$\mathcal{H}_c = \mathcal{C}\mathbf{S}_i \; \mathbf{r}_{ij}. \tag{10}$$

Where $\mathbf{r}_{ij} = \mathbf{r}_j - \mathbf{r}_i$ is the separation of the atoms and C is a parameter to control the strength of the coupling. Using this Karakurt *et al.* demonstrated that this coupling causes a damping of the uniform precession mode. Beaujouan *et al.* [63] propose a different type of coupling based on a two site anisotropy which takes the form of pseudo-dipole interaction.

$$\mathcal{H}_c = K(\mathbf{r}_{ij})\left((\hat{\mathbf{r}}_{ij} \; \mathbf{S}_i)(\hat{\mathbf{r}}_{ij} \cdot \mathbf{S}_j) - \frac{\mathbf{S}_i \cdot \mathbf{S}_j}{3} \right). \tag{11}$$

In this case the coupling strength, K, depends on the separation of the atoms and requires specific parametrisation from *ab initio*. As discussed in the literature this form of coupling arises from the spin-orbit interaction of the electrons and thus is more physically justifiable but is still not exact. With this Beaujouan *et al.* are able to show that energy can be transferred between the systems and an equilibrium temperature is obtained. It is clear that by incorporating lattice dynamics into the ASD model various effects which are treated phenomenologically are present. However these still require a high level of empirical parametrisation for both the atomic bonding and the spin-lattice coupling.

Finally, we consider briefly one further aspect of the use of fixed spin models such as the LL equation, specifically the classical nature of the spin. This leads to a disparity between the simulated and experimental temperature dependent magnetization curves [64]. At the macroscopic level the temperature dependent magnetization is well fitted by the phenomenological equation proposed by Kuz'min [64]. However, the Kuz'min equation merely describes the form of the curve with little relation to the microscopic interactions within the material which determine fundamental properties such as the Curie temperature. Ideally one would perform 3D quantum Monte Carlo simulations [65], but, although this is possible for small numbers of atoms, for larger ensembles the multiscale approach using atomistic models parameterized with *ab-initio* information remains the only feasible approach to connect the quantum and thermodynamic worlds. Evans *et al.* [66] have proposed a scaling approach which maps classical to quantum spin models. The scaling recognises that, although the classical treatment finds the correct magnon energies, the distinction between classical and quantum models results from the particular statistical properties of each approach. While quantum systems obey Bose–Einstein statistics, leading to the Bloch $T^{3/2}$ law at low temperatures, the classical Boltzmann statistics gives rise to a finite slope of the magnetization at low temperatures. In Ref. 66 the existence of a simple relation between classical and quantum temperature-dependent magnetization at low temperatures is demonstrated. The temperature-dependent magnetization is represented in the simplest form arising from a straightforward interpolation of the Bloch law and critical behavior given by the Curie–Bloch equation

$$m(\tau) = (1 - \tau^\alpha)^\beta \tag{12}$$

where α is an empirical constant and $\beta = 1/3$ is the critical exponent. Evans *et al.* [66] then use the classical spin model simulations to determine the critical exponent β and then find α by fitting the classical model predictions to experimental data. This leads to a mapping from a "simulation temperature" to the real temperature. It was shown that this approach gives excellent agreement with experiment [39] for the demagnetization of Ni following an ultrafast laser pulse.

5. Conclusion

The use of the LL equation in ASD models of magnetic materials has been described. The introduction of the LL equation, in its stochastic form, is the basis of a powerful approach to ultrafast spin dynamics. In particular, ASD simulations demonstrate the important thermodynamic contribution to laser-induced ultrafast processes. The models demonstrate a new, so-called linear reversal mechanism which is the path to ultrafast reversal. Also predicted is the phenomenon of TIMS, which is currently under extensive investigation and holds the promise of application in future devices requiring fast switching. The success of the LL equation in this framework is remarkable. While further investigations of the energy transfer mechanisms at the quantum level should be carried out to improve the physical understanding of damping, ASD methods based on the LL equations are likely to have an important role in understanding the physics of magnetic phenomena, not only at short timescales and elevated temperatures, but also on lengthscales where the micromagnetic formalism is not appropriate.

1. *Monte Carlo Methods in Statistical Physics*, K. Binder (ed.) Springer-Verlag, Berlin (1979), p. 204.

2. U. Nowak, R.W. Chantrell, and E.C. Kennedy. *Phys. Rev. Lett.* **84**, 163 (2000).

3. R. Koctema and A. Berkowitz, *Phys. Rev. B* **59**, 6321 (1999).

4. C. Mitsumata, A. Sakuma, and K. Fukamichi, *Phys. Rev. B* **68**, 014437 (2003).

5. U. Nowak, R. Wieser, O.N. Mryasov, K. Guslienko, and R.W. Chantrell, *Phys. Rev. B* **72**, 172410 (2005).

6. E. Boerner, O. Chubykalo-Fesenko, R. Chantrell, O. Heinonen, and O. Mryasov, *IEEE Trans. Magn.* **41**, 936 (2005).

7. B. Skubic, J. Hellsvik, L. Nordstrom, and O. Eriksson *J. Phys.: Condens. Matter* **20**, 315203 (2008).

8. W.F. Brown, Jr., *Micromagnetics Interscience*, New York (1963).

9. G. Grinstein and R.H. Koch, *Phys. Rev. Lett.* **90**, 207201 (2003).

10. E. Martinez, L. Lopez-Diaz, L. Torres, and O. Alejos, *IEEE Trans. Magn.* **39**, 2522 (2003).

11. T.W. McDaniel, *J. Phys.: Condens. Matter* **17**, R315 (2005).

12. E. Rottmayer, S. Batra, D. Buechel, W.A. Challenger, J. Hohlfeld, Y. Kubota, L. Li, B. Lu, C. Mihalcea, K. Mountfield, K. Pelhos, C. Peng, T. Rausch, M.A. Siegler, D. Weller, and X.M. Yang, *IEEE Trans. Magn.* **42**, 2417 (2006).

13. K. Schwarz, P. Mohn, P. Blaha, and J. Kobler, *J. Phys. F* **14**, 2659 (1984).

14. R.F.L. Evans, W.J. Fan, P. Chureemart, T.A. Ostler, M.O.A. Ellis, and R.W. Chantrell, *J. Phys.: Condens. Matter* **26**, 103202 (1984).

15. O. Mryasov, U. Nowak, K. Guslienko, and R.W. Chantrell, *Europhys. Lett.* **69**, 805 (2005).

16. L. Szunyogh, L. Udvardi, J. Jackson, U. Nowak. and R.W. Chantrell, *Phys. Rev. B* **83**, 024401 (2011).

17. T.A. Ostler, R. Evans, R.W. Chantrell, U. Atxitia, O. Chubykalo-Fesenko, I. Radu, R. Abrudan, F. Radu, A. Tsukamoto, A. Itoh, A. Kirilyuk, Th. Rasing, and A. Kimel, *Phys. Rev. B* **84**, 024407 (2011).

18. R.F.L. Evans, D. Givord, R. Cuadrado, M.I.J. Probert, T. Shoji, A. Manabe, M. Yano, G. Hrkac, T. Schrefl, and R.W. Chantrell (submitted).

19. G. Kresse and J. Furthmuller, *Phys. Rev. B* **54**, 11169 (1996).

20. J.M. Soler, E. Artacho, J.D. Gale, A. García, J. Junquera, P. Ordejón, and D. Sánchez Portal, *J. Phys.: Condens. Matter* **14**, 2745 (2002).

21. J. Zabloudil, R. Hammerling, L. Szunyogh, and P. Weinberger, *Electron Scattering in Solid Matter*, Springe, Berlin (2005).

22. H. Ebert, D. Ködderitzsch, and D. Minár, *Rep. Prog. Phys.* **74**, 096501 (2011).

23. M.I. Katsnelson and A.I. Lichtenstein, *Phys. Rev. B* **61** 8906 (2000).

24. M. Pajda, J. Kudrnovsky, I. Turek, V. Drchal, and P. Bruno, *Phys. Rev. B* **64**, 174402 (2001).

25. A. Liecntenstein, M. Katsnelson, V. Antropov and V. Gubanov, *J. Magn. Magn. Mater.* **67**, 65 (1987).

26. N. Kazantsev, D. Hinzke, R.W. Chantrell, U. Atxitia, and O. Chubykalo-Fesenko, *Phys. Rev. B* **77**, 184428 (2008).

27. O.N. Mryasov, U. Nowak, K.Y. Guslienko, and R.W. Chantrell, *Europhys. Lett.* **69**, 805 (2005).

28. M.O.A. Ellis and R.W. Chantrell, *Appl. Phys. Lett.* **106**, 162407 (2015).

29. O. Hovorka, S. Devos, Q. Coopman, W.J. Fan, C.J. Aas, R.F.L. Evans, Xi Chen, G. Ju, and R.W. Chantrell, *Appl. Phys. Lett.* **101**, 052406 (2012).

30. A. Lyberatos, D. Weller, and G.J. Parker, *J. Appl. Phys.* **114**, 233904 (2013).

31. A. Lyberatos, D. Weller, G.J. Parker, and B.C. Stipe, *J. Appl. Phys.* **112**, 113915 (2012).

32. E.R. Callen and H.B. Callen, *J. Phys. Chem. Solids* **27**, 1271 (1966).

33. J.-U. Thiele, K.R. Coffey, M.F. Toney, J.A. Hedstrom, and A.J. Kellock, *J. Appl. Phys.* **91**, 6595 (2002).

34. S. Okamoto, N. Kikuchi, O. Kitacami, T. Miyazaki, Y. Shimada, and K. Fukamichi, *Phys. Rev. B* **66**, 24413 (2002).

35. A. Lyberatos, D.V. Berkov, and R.W. Chantrell, *J. Phys: Condens. Matter* **5**, 8911 (1993).

36. W.F. Brown, Jr., *Phys. Rev.* **130**, 1677 (1963).

37. J.L. Garciá-Palacios and F.J. Lazaro, *Phys. Rev. B* **58**, 14937 (1998).

38. D.V. Berkov, *IEEE Trans. Magn.* **38**, 2489 (2002).

39. E. Beaurepaire, J.-C. Merle, A. Daunois, and J.-Y. Bigot, *Phys. Rev. Lett.* **76**, 4250 (1996).

40. C.D. Stanciu, F. Hansteen, A.V. Kimel, A. Kirilyuk, A. Tsukamoto, A. Itoh, and Th. Rasing, *Phys. Rev. Lett.* **99**, 047601 (2007).

41. K. Vahaplar, A.M. Kalashnikova, A.V. Kimel, D. Hinzke, U. Nowak, R. Chantrell, A. Tsukamoto, A. Itoh, A. Kirilyuk, and Th. Rasing, *Phys. Rev. Lett.* **103**, 117201 (2009).

42. P. Nieves, U. Atxitia , R.W. Chantrell, and O. Chubykalo-Fesenko, *Fiz. Nizk. Temp.* **41**, 949 (2015) [*Low Temp. Phys.* **41**, No. 9 (2015)].

43. N. Kazantseva, D. Hinzke, R.W. Chantrell, and U. Nowak *Europhys. Lett.* **86**, 27006 (2009).

44. C.-H. Lambert, S. Mangin, B.S.D.C.S. Varaprasad, Y.K. Takahashi, M. Hehn, M. Cinchetti, G. Malinowski, K. Hono, Y. Fainman, M. Aeschlimann, and E.E. Fullerton, *Science* **345**, 1337 (2014).

45. J. Chen, D. Tzou, and J. Beraun, *Int. J. Heat and Mass Transfer* **49**, 307316 (2006).

46. I. Radu, K. Vahaplar, C. Stamm, T. Kachel, N. Pontius, H. A. Drr, T.A. Ostler, J. Barker, R.F.L. Evans, R.W. Chantrell, A. Tsukamoto, A. Itoh, A. Kirilyuk, Th. Rasing, and A.V. Kimel, *Nature* **472**, 205 (2011).

47. T.A. Ostler, J. Barker, R.F.L. Evans, R. Chantrell, U. Atxitia, O. Chubykalo-Fesenko, S. El Moussaoui, L. Le Guyader, E. Mengotti, L.J. Heyderman, F. Nolting, A. Tsukamoto, A. Itoh, D. Afanasiev, B.A. Ivanov, A.M. Kalashnikova, K. Vahaplar, J. Mentink, A. Kirilyuk, Th. Rasing, and A.V. Kimel, *Nat. Commun.* **3**, 666 (2012).

48. A.R. Khorsand, M. Savoini, A. Kirilyuk, A.V. Kimel, A. Tsukamoto, A. Itoh, and Th. Rasing, *Phys. Rev. Lett.* **108**, 127205 (2012).

49. J.H. Mentinck, J. Hellsvik, D.V. Afanasiev, B.A. Ivanov, A. Kirilyuk, A.V. Kimel, O. Eriksson, M.I. Katsnelson, and Th. Rasing, *Phys. Rev. Lett.* **108**, 057202 (2012).

50. U. Atxitia, T. Ostler, R.F.L. Evans, R.W. Chantrell, and O. Chubykalo-Fesenko, *Phys Rev. B* **87**, 224417 (2013).

51. J. Barker, U. Atxitia, T.A. Ostler, O. Hovorka, O. Chubykalo-Fesenko, and R.W. Chantrell, *Sci. Rep.* **3**, 3262 (2013).

52. R.F.L. Evans, T.A. Ostler, R.W. Chantrell, I. Radu, and Th. Rasing, *Appl. Phys. Lett.* **104**, 082410 (2014).

53. R.F.L. Evans, R.W. Chantrell, U. Nowak, A. Lyberatos, and H.-J. Richter, *Appl. Phys. Lett.* **100**, 102402 (2012).

54. K. Capelle and B.L. Gyorffy, *Europhys. Lett.* **61**, 354 (2003).

55. K. Blum, *Density Matrix Theory and Applications*, Plenum Press, New York (1981).

56. R. Wieser, *Eur. Phys. J. B* **88**, 77 (2015).

57. U. Atxitia, O. Chubykalo-Fesenko, R.W. Chantrell, U. Nowak and A. Rebei, *Phys. Rev. Lett.* **102**, 057203 (2009).

58. K. Miyazaki and K. Seki, *J. Chem. Phys.* **108**, 7052 (1998).

59. J.M. Sancho and M. San Miguel, *Phys. Rev. A* **26**, 1589 (1982).

60. P.-W. Ma, C. Woo, and S. Dudarev, *Phys. Rev. B* **78**, 024434 (2008).

61. P.-W. Ma, S. Dudarev, and C. Woo, *Phys. Rev. B* **85**, 184301 (2012).

62. S. Karakurt, R. Chantrell, and U. Nowak, *J. Magn. Magn. Mater.* **316**, 280 (2007).

63. D. Beaujouan, P. Thibaudeau, and C. Barreteau, *Phys. Rev. B* **86**, 174409 (2012).

64. M.D. Kuzmin, *Phys. Rev. Lett.* **94**, 107204 (2005).

65. A.W. Sandvik and J. Kurkijarvi, *Phys. Rev. B* **43**, 5950 (1991).

66. R.F.L. Evans, U. Atxitia, and R.W. Chantrell, *Phys. Rev. B* **91**, 144425 (2015).